C201 Viscous Flow and Turbulence

Lecture 4

Part 1: RSM models and scale resolving methods

Luca di Mare

St John's College

1 Beyond the Boussinesq's hypothesis

In the previous lecture we have examined in detail the behaviour of linear eddy viscosity models. We have seen that these models tend to work best at high Reynolds numbers and in mild pressure gradients. In these conditions their predictions for relatively simple flows agree well with each other and with available experimental data or accurate numerical data. We have also seen that the intermediate quantities of the models (e.g. eddy viscosities) may differ widely but still result in no more than subtle differences in macroscopic flow parameters such as mean flow profiles and Reynolds stress distribution.

Linear eddy viscosity models have enjoyed considerable popularity because of their adequate performance in most flows, their relatively low computational cost and the ease (in most cases) with which boundary conditions can be prescribed from scant information about the flow.

These favourable characteristics come despite their fairly shaky foundations in Boussinesq's hypothesis. At the start of last lecture we mentioned that Boussinesq's hypothesis is not strictly met even in simple flow. As an example, in turbulent channels and boundary layers the normal Reynolds stresses are not isotropic but

$$\overline{u'^2}:\overline{v'^2}:\overline{w'^2} = 1.0:0.4:0.6$$

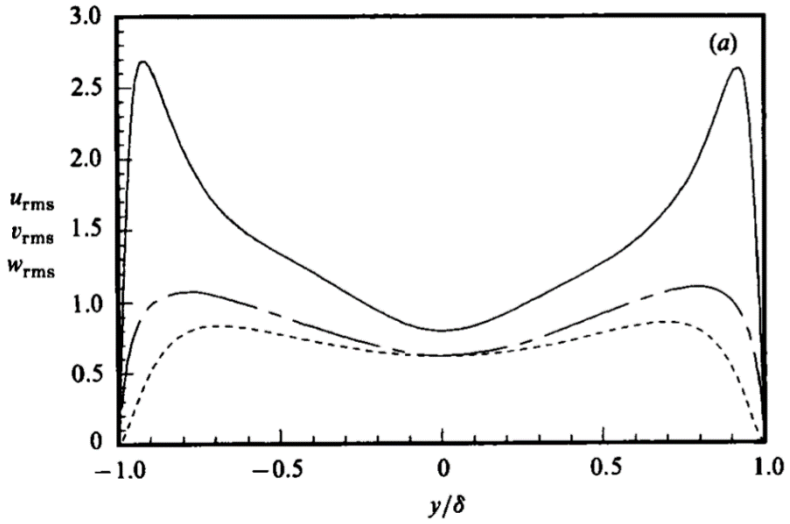

Figure 1: velocity RMS in turbulent channel flow from Kim, J., Moin, P., & Moser, R. (1987). Turbulence statistics in fully developed channel flow at low Reynolds number. *Journal of Fluid Mechanics, 177*, 133-166.

as can be seen from Figure 1. Most eddy viscosity models assume instead

$$\overline{u'^2} = \overline{v'^2} = \overline{w'^2} = \frac{2}{3}k$$

as required by Boussinesq's hypothesis.

In boundary layers past flat surfaces, the anisotropy of the Reynolds stress is not particularly consequential, but it becomes important in flows through ducts with square or polygonal section. In these cases, the anisotropy of the Reynolds stress results in source terms in the vorticity transport equation. The source terms are proportional to the differences between normal Reynolds stresses (Brundrett, E., & Baines, W. (1964). The production and diffusion of vorticity in duct flow. *Journal of Fluid Mechanics, 19*(3), 375-394). The source terms in the vorticity transport equation result in the formation of secondary flow patterns in the plane orthogonal to the flow direction (see Figure 2). These flow patterns alter the friction, heat and mass transfer properties of the flow, but are completely absent from predictions with linear eddy viscosity models.

Findings such as these have encouraged the search for a better approximation of the Reynolds stress tensor.

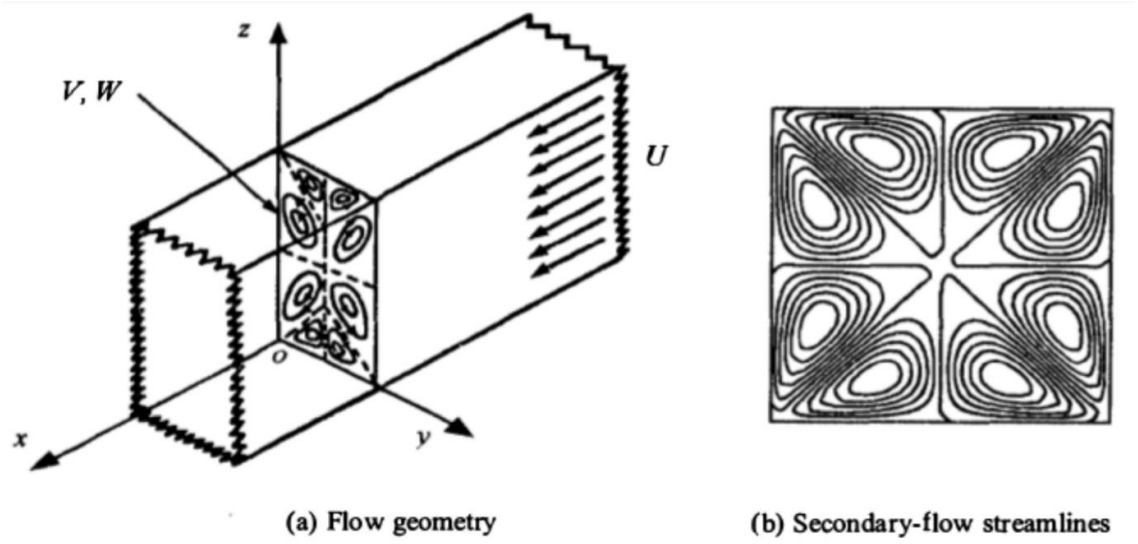

Figure 2: secondary flow patterns in the plane orthogonal to the mean flow due to Reynolds stress anisotropy.

2 Reynolds stress transport model

We have seen that the transport equation for the k variable in the $k-\varepsilon$ and $k-\omega$ models is at least loosely based on the TKE transport equation we derived in the first lecture of this module. The starting point for Reynolds stress transport models is the observation that a transport equation can be written for the whole Reynolds stress tensor and that such transport equation can be used as the bases for models that estimate directly the independent components of the Reynolds stress.

2.1 The Reynolds stress budget

A budget equation for the Reynolds stress can be derived in a fashion similar to the derivation of the TKE budget, with the exception that the momentum equation for the i-th velocity perturbation needs to be multiplied by the j-th velocity perturbation and vice-versa (see question 8 in the example sheet).

The transport equation for the component

$$\tau_{lm} = \overline{u_l' u_m'}$$

is

$$\underbrace{U_j \frac{\partial \tau_{lm}}{\partial x_j}}_{\text{Convection}} = \underbrace{\Pi_{lm}}_{\substack{\text{Pressure terms} \\ \text{(see below)}}} - \underbrace{\nu \frac{\partial^2 \tau_{lm}}{\partial x_j \partial x_j}}_{\text{Viscous diffusion}} - \underbrace{\epsilon_{lm}}_{\text{Dissipation}} - \underbrace{\frac{\partial}{\partial x_j} \overline{u_j' u_l' u_m'}}_{\text{Turbulent diffusion}} - \underbrace{\left(\tau_{li} \frac{\partial u_m}{\partial x_i} + \tau_{mi} \frac{\partial u_l}{\partial x_j} \right)}_{\text{Production}}$$

where

$$\Pi_{lm} = \underbrace{- \overline{p' \left(\frac{\partial u_l}{\partial x_m} + \frac{\partial u_m}{\partial x_l} \right)}}_{\text{Pressure strain correlatin}} \underbrace{- \frac{\partial}{\partial x_l} \overline{p' u_m'} - \frac{\partial}{\partial x_m} \overline{p' u_l'}}_{\text{Pressure diffusion}}$$

$$\epsilon_{lm} = \nu \overline{\left(\frac{\partial u_l'}{\partial x_m} + \frac{\partial u_m'}{\partial x_l} \right)^2}$$

While promising, the Reynolds stress budget is by itself no more useful than the TKE budget in deriving a turbulence model. We see immediately that while certain terms depend only on the Reynolds stress itself and the mean velocity (e.g. the viscous diffusion, the convection and the production), others depend on quantities that are not accessible via the RANS equations, such as the pressure-velocity correlations, the turbulent diffusion or the dissipation. In essence the Reynolds stress budget has the same closure problem as the RANS equations.

2.2 Reynolds stress transport models

There have been attempts to model the Reynolds stress budget. The first attempt was by Rotta (1959), followed by Hanjalic and Launder (1972). The first practical Reynolds stress transport model was the Launder Reece Rodi (LRR) model (1974). The LRR model approximates pressure-velocity correlations via theoretical estimates, it approximates turbulent diffusion through an eddy viscosity and uses the ε equation from the $k - \varepsilon$ model to determine the dissipation rate.

The LRR model requires the solution of additional partial differential equations for a three-dimensional flow: 6 independent equations of the Reynolds stress tensor and the ε equation.

2.3 Algebraic RSM closures

Reynolds stress transport models such as the LRR model are quite difficult to program and to handle computationally. An alternative could be to use information from an ordinary 2-equation model but then to apply a more flexible constitutive

- $\tau_{ij} = -\rho k(a_{ij} + \frac{2}{3}\delta_{ij})$
- a_{ij} is a polynomial of S_{ij} and Ω_{ij}

$$S_{ij} = \frac{t}{2}(\frac{\partial u_j}{\partial x_i} + \frac{\partial u_i}{\partial x_j} - \frac{2}{3}\delta_{ij}\frac{\partial u_k}{\partial x_k}) \quad (3)$$

$$\Omega_{ij} = \frac{t}{2}(\frac{\partial u_i}{\partial x_j} - \frac{\partial u_j}{\partial x_i}) \quad (4)$$

$$t = max(\frac{1}{C_\mu \omega}, 6\sqrt{\frac{\mu}{C_\mu \rho k \omega}}) \quad (5)$$

- a_{ij} is formulated as:

$$a_{ij} = \beta_1 T_{1,ij} + \beta_3 T_{3,ij} + \beta_4 T_{4,ij} + \beta T_{6,ij} + \beta_9 T_{9,ij} \quad (6)$$

$$T_{1,ij} = S_{ij} \quad (18)$$

$$T_{3,ij} = \Omega_{ik}\Omega_{kj} - \frac{1}{3}H_\omega \delta_{ij} \quad (19)$$

$$T_{4,ij} = S_{ik}\Omega_{kj} - \Omega_{ik}S_{kj} \quad (20)$$

$$T_{6,ij} = S_{ik}\Omega_{kl}\Omega_{lj} + \Omega_{ik}\Omega_{kl}\Omega_{lj} - \frac{2}{3}H_{s\omega}\delta_{ij} - H_\omega S_{ij} \quad (21)$$

$$T_{9,ij} = \Omega_{ik}\Omega_{kl}\Omega_{lm}\Omega_{mj} - \Omega_{ik}\Omega_{kl}S_{lm}\Omega_{mj} + \frac{1}{2}H_\omega(S_{ik}\Omega_{kj} - \Omega_{ik}S_{kj}) \quad (22)$$

Figure 3: some (!) of the terms of the baseline EARSM model

relation between the Reynolds stress and the shear rate tensor S_{ij} and the vorticity tensor Ω_{ij}. Algebraic RSM closures do just that. Usually the constitutive relation is a tensor polynomial comprising the tensors S_{ij} and Ω_{ij}. The constitutive relations of ARSM models can be quite cumbersome: Figure 3 shows some of the terms in the baseline EARSM model.

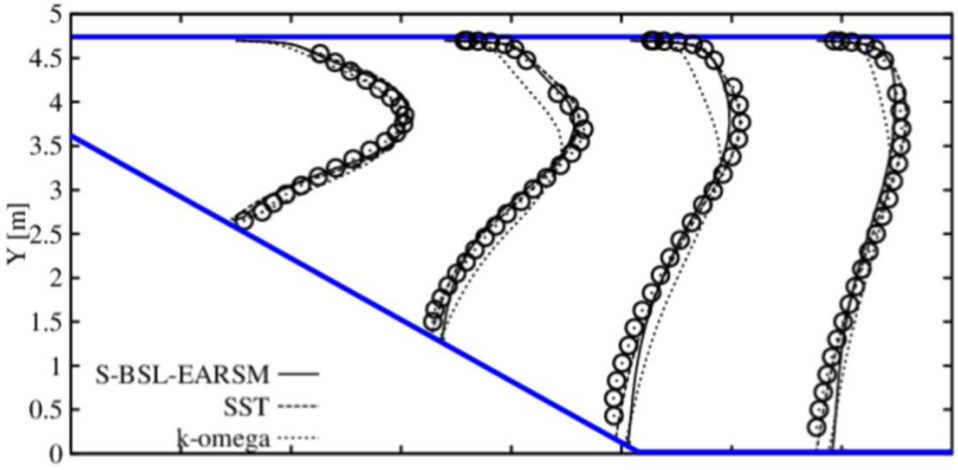

Figure 4: velocity profiles in a two-dimensional diffuser with the $k-\omega$ model (Wilcox and SST) and the SBSL-EARSM model.

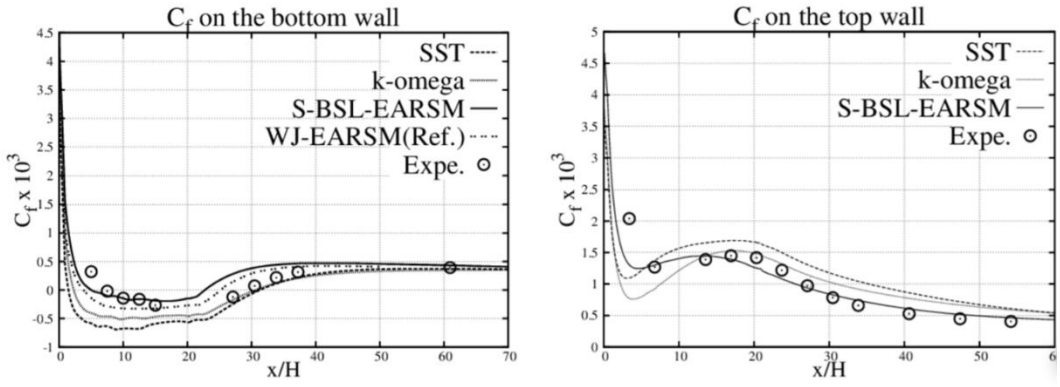

Figure 5: friction coefficients in two-dimensional diffuser. Comparison of experiments, $k-\omega$ model (Wilcox and SST) and the SBSL-EARSM model.

2.4 Performance of RSM models

We examine the performance of RSM models for two diffusers, a two-dimensional case and a three-dimensional case. A diffuser is a simple model for devices like exhaust systems, intakes and compressor passages.

2.4.1 Two-dimensional diffuser

Results for a two-dimensional diffuser are shown in Figure 4 and Figure 5. The results shown are velocity profiles and friction coefficients comparing predictions obtained by the $k-\omega$ model (both Wilcox and SST) and the SBSL-EARSM model. Also shown are experimental data.

The differences in the velocity profiles are relatively subtle but they correspond to notable differences in c_f: the models predict different separation and reattachment locations and different sizes of the separated flow.

2.4.2 Three-dimensional diffuser

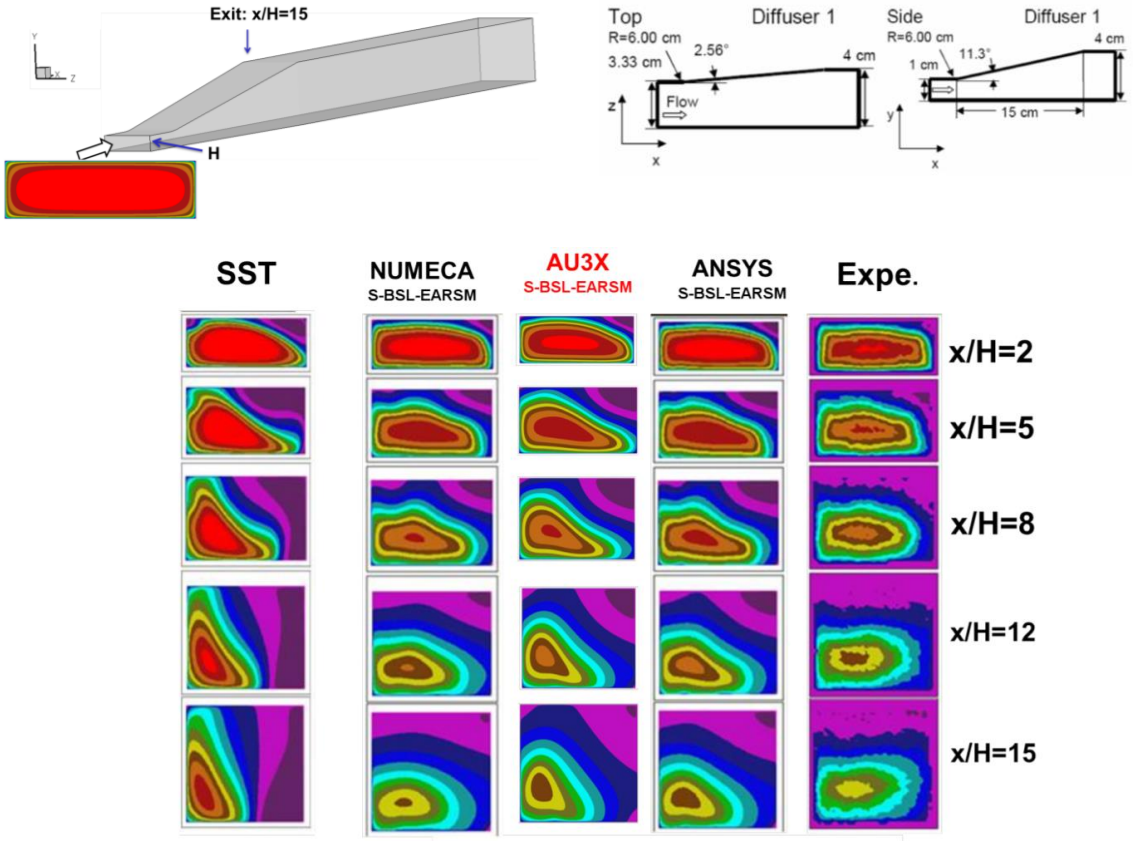

Figure 6: configuration (top) and axial velocity contours for the three-dimensional diffuser. The data set AU3X SBSL-EARSM was obtained by your lecturer's research group.

Three dimensional diffusers are of considerable practical interest because they have flow features similar to those encountered in intakes for high-speed aircraft, compressor passages, exhaust systems for industrial gas turbines.

The the diffuser is essentially a diverging square duct, with two adjacent straight walls and two diverging walls, set at different angles. Because of the different setting angle of the diverging walls, the flow slows down in different measure on the two corresponding sides of the diffuser. The end result is a mean velocity distribution skewed towards the corner between the straight walls.

The axial velocity distribution on planes orthogonal to the mean flow direction is shown in Figure 6. The data being compared are measurements against numerical predictions obtained with the $k-\omega$ model and four different implementation of the SBSL-EARSM model. As expected, the unaugmented $k-\omega$ model produces a qualitatively incorrect flow distribution. This outcome was expected on the grounds of the inability of linear eddy viscosity models to predict secondary flows in square ducts. The EARSM models are generally closer to the experimental data and show the flow clustering on the correct side of the duct. More surprisingly, the four implementations of the SBLS-EARSM model produce visibly different results. This shows that the turbulence models are sensitive to the discretization and that these two aspects of numerical predictions cannot really be assessed in isolation.

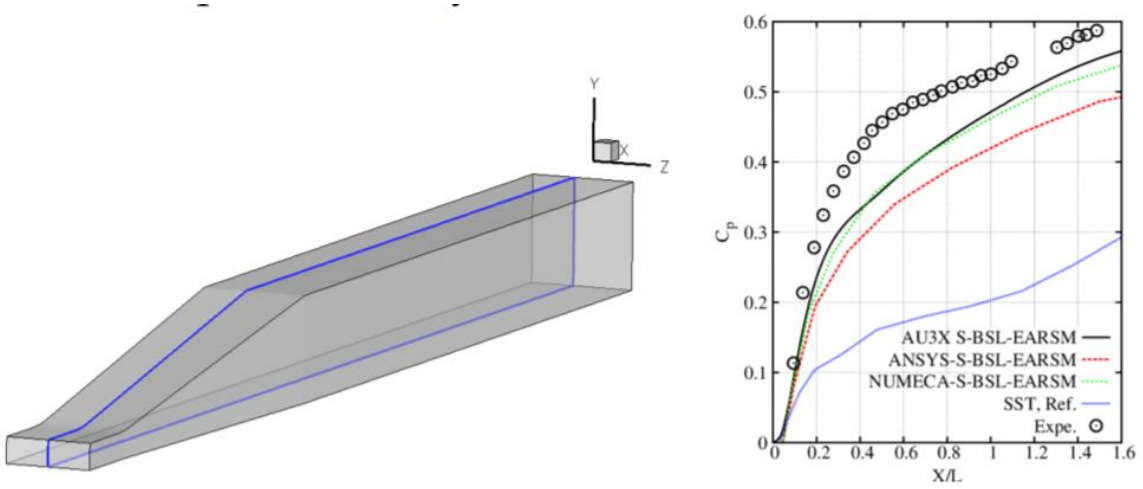

Figure 7: pressure coefficient along the upper wall of the three-dimensional diffuser.

3 Direct Numerical Simulation (DNS)

DNS and other scale resolving techniques do not attempt to solve the RANS equations but solve directly the time-dependent Navier-Stokes equations, in some approximate form. The DNS technique does not alter the equations and relies on computational power to resolve all the length- and time-scales active in a flow.

DNS calculations usually require very accurate numerical methods because these reduce the resolution requirements and make the calculations more affordable.

We can obtain estimates for the cost of a DNS using Kolmogorov's theory. Since a DNS needs to resolve all the scales of motion, the grid spacing is set by the

Kolmogorov's scale η. The domain size, on the other hand, is set by the integral length scale ℓ.

If we are trying to simulate a cubic domain, the number of cells along each side is

$$N = \frac{\ell}{\eta} = Re_t^{3/4} = \left(\frac{u'\ell}{\nu}\right)^{3/4}$$

Where we have made use of the ratio between Kolmogorov's and integral scale (See lecture 2).

The total number of cells is N^3:

$$N^3 = Re_t^{\frac{9}{4}}$$

Because the simulation is unsteady, we also need to select a time step. The time step for unsteady simulations is usually chosen so that

$$\frac{U_\infty}{\Delta x}\Delta t = const$$

$$\Delta x = \ell/N$$

Therefore

$$\frac{U_\infty}{\ell} N\Delta t = const$$

$$\Delta t \propto \frac{1}{N}\frac{\ell}{U_\infty}$$

The number of time steps needed scales with the ratio

$$T = \frac{\ell}{U_\infty \Delta t} \propto N$$

So the final cost of the simulation is

$$TN^3 = N^4 \propto Re_t^3$$

We see that the cost of a DNS simulation grows very rapidly with the turbulence Reynolds number. It is this unfavourable scaling that limits the applicability of DNS to very large Reynolds numbers.

4 Large Eddy Simulations (LES)

Large Eddy Simlation (LES) is a technique based on Kolmogorov's 1941 theory

LES acknowledges that the energy of turbulence is distributed across a range of wave- and time-scales. The smaller scales are ruled by the K41 theory. This makes them universal and easier to model. LES tries to exploit this property by resolving the large scales of motion and modelling the smaller scale.

Large eddies can be explicitly solved by using fine enough mesh to capture the large eddies. Small eddies are implicitly taken into account by modelling them using so called subgrid-scale models (SGS)

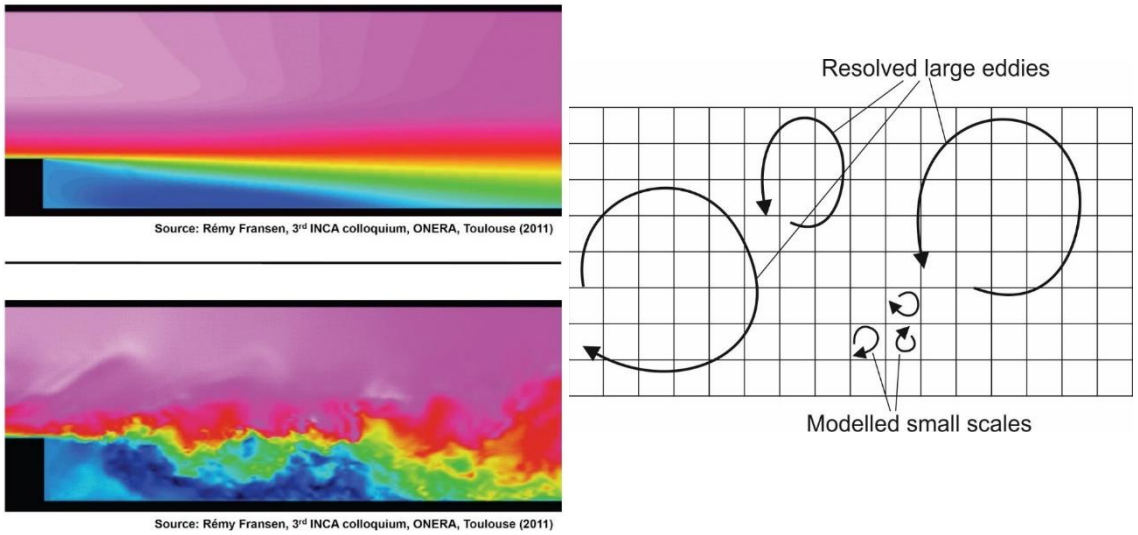

Figure 8: LES resolves large scales and models small scales.

Because LES calculations dispense with the small scales, they can be considerably cheaper than DNS simulations of the same flow. The scale separation argument underpinning LES fails in proximity of a wall because, as we have seen studying turbulent channel flows, the size of turbulent eddies is bound to the distance from the wall. As a consequence, LES calculations attempting to resolve turbulent structures near a wall can be prohibitively expensive because of the need to resolve small structures. This issue has encouraged the development of approximate boundary conditions that allow realistic values for the wall shear stress to be included in the simulation even if the turbulent structures near the wall are not explicitly resolved.

5 Reynolds stress transport models: checklist

The shortcomings of linear eddy viscosity models become apparent when the anysotropy of the Reynolds stress tensor influences the mean flow, as it does in the flow in square ducts.

One way of overcoming the shortcomings of linear eddy viscosity models is to model the transport equation for the Reynolds stress tensor. This equation has similar structure to the TKE budget equation and it suffers from similar closure problems. The Launder Reece Rodi model is an example of Reynolds Stress Transport model because it attempts to model the Reynolds stress budget. The model is very complex to program. A – marginally – simpler alternative is represented by Algebraic Reynolds Stress Models where the transport equations are those for common two-equation models, but the constitutive relation between mean flow and Reynolds

stress is modified. This relation usually takes the shape of a matrix polynomial involving products of the shear tensor and the rotation tensor.

Scale resolving simulations like LES and DNS forgo attempts to solve the Reynolds-Averaged flow and instead operate directly on the unsteady Navier-Sokes equations. DNS uses the equations with no modelling and resolves all scales of motion, whereas LES models the smallest scales and only resolves the largest.